DOI 10.1007/s11223-021-00294-y
Strength of Materials, Vol. 53, No. 2, March, 2021

EXPERIMENTAL STUDY ON THE SURFACE PROPERTY CHANGES OF ALUMINUM ALLOY AND STAINLESS STEEL AFTER IMPINGEMENT WITH SUBMERGED CAVITATION JET

Y. F. Yang,[a] W. D. Shi,[a,1] W. Li,[b] S. P. Chen,[b] W. Q. Zhang,[b] and B. Pan[c]

UDC 539.4

With the development of green manufacturing technology, high-pressure cavitation water jet cleaning and shot peening technologies are gradually replacing traditional high-pollution processes. To improve the processing quality and efficiency, three types of metal alloys are impinged with cavitation jet under different processing parameters. By changing the impact time, impact target distance and nozzle form, the impact erosion and peening effects of high-pressure water cavitation jets are studied. The surface micro-topographies of the metal surface under different erosion stages are observed via SEM images. The mechanical behavior, including micro-hardness, residual stress and grain cell structure of the alloy, related to different processing parameters is investigated. It is found that, for the low-strength material Al1060, a cavitation jet can cause its surface damage in a very short time. The stand-off distance has a significant effect on the impact efficiency, and the shape of the nozzle outlet also affects the impact performance. Mechanical properties of Al6061 and 304-stainless steel can be improved under the appropriate impact time. If the processing time and other parameters are properly controlled, the hardness of the metal surface layer rises, and residual compressive stress with a certain depth can be induced.

Keywords: cavitation jet, nozzle, hardness, residual stress, surface shape.

Introduction. In recent years, high-pollution equipment cleaning processes such as shot blasting and shot peening are gradually eliminated, and the high-pressure water jet is increasingly used to clean and cut large-scale offshore engineering and chemical equipment [1–3]. The requirements of ultra-high pressure usually bring expensive equipment, high energy consumption and safety risks. One way to improve the efficiency of the water jets without increasing the pressure is the application of the abrasive jet technics [4–6]. At present, a new way to reduce the working pressure of high-pressure water jets is to make use of the cavitation clouds generated in the shear layer of the submerged jets. Howard et al. [7] developed cavitation water jet equipment for ocean cleaning. In the experiment, epoxy vinyl was used as the coating to spray on the surface of the offshore platform components. When the cleaning process was performed at a rate of 16 m^2/h, the coating on the surface of the equipment was completely cleared, and the equipment required only 22 hp.

Soyama [8–13] put forward the idea of applying the local high-energy shock wave during the collapse of cavitation to the field of metal peening when studying cavitation jets, and carried out a lot of research on the high-pressure water peening process. They used submerged cavitation jets, combined submerged jets, and submerged jets in the air to perform peening tests on different material patterns and mechanical parts, and compared the results

[a]College of Mechanical Engineering, Nantong University, Nantong, China ([1]wdshi@ujs.edu.cn). [b]Research Center of Fluid Machinery Engineering and Technology, Jiangsu University, Zhenjiang, China. [c]Shandong Xinchuan Mine Electrical and Mechanical Equipment Co., Ltd, Jining, China. Translated from Problemy Prochnosti, No. 2, pp. 159 – 169, March – April, 2021. Original article submitted January 28, 2020.

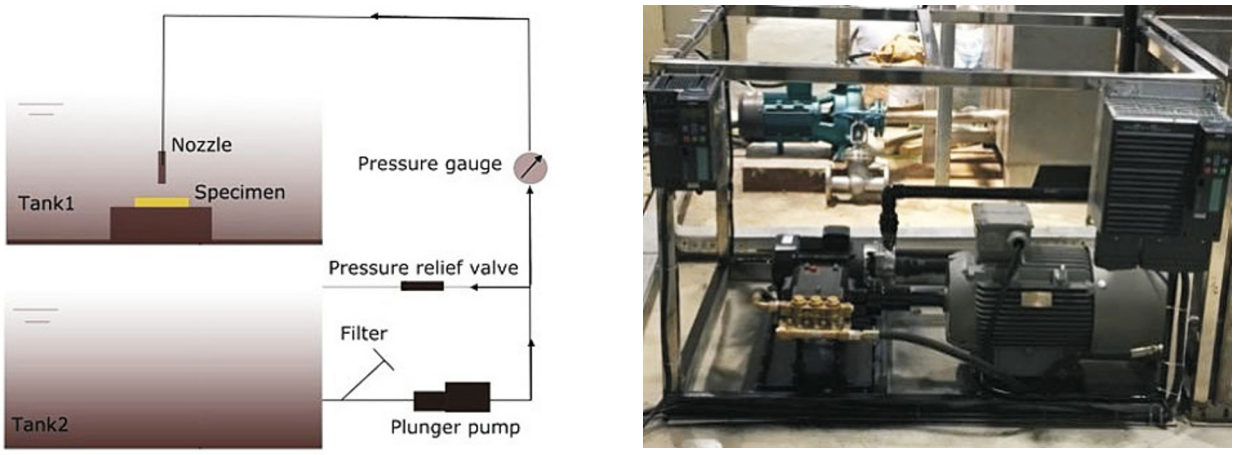

a b

Fig. 1. Test platform for high-pressure submerged jet: (a) schematic diagram; (b) photo of test platform.

of the shot peening test with the traditional steel ball peening and laser peening. It has been found that cavitation water jet peening has a better strengthening effect, and has the following advantages compared with the traditional shot peening: (1) The force is uniformly loaded when the cavitation collapses, and the surface roughness before and after shot peening does not increase significantly. (2) Very high local impact pressure can be generated when the cavitation collapses; a thick residual stress layer can be formed on the metal surface after the impact, and the surface grain can be refined efficiently. (3) The working medium is clean water, and no pollution and emissions, which is environmentally friendly and low cost.

To improve the effect of cavitation water jet peening, Macodiyo and Soyama [14] used orthogonal experiments to optimize the parameters of cavitation water jet, and found that cavitation number is the main factor affecting the peening effect. Sekine and Soyama [15] used the eddy current method to evaluate the surface properties of steel before and after the cavitation water jet impact. It was found that the depth of residual stress and the degree of grain refinement were greatly affected by the processing time. In order to avoid distraction created by excessive impact corrosion damage, choosing the appropriate impact time is critical to the peening process. Marcon et al. [16] studied the effect of nozzle size on the peening performance of cavitation water jets and found that when the nozzle size increases, the residual stress obtained from peening will be significantly improved, and the required peening time is also obviously reduced. In order to further improve the effect of cavitation water jet peening, Ijiri et al. [17] designed a cyclone structure at the outlet of the high-pressure nozzle. This structure uses the low-pressure area generated by high-speed flow when the submerged high-pressure water jet works entraining the liquid from the outside and interacting with the cavitation jet effectively increases the number of cavitation bubbles and the impact force when the cavitation collapses.

However, the existing research of jet peening and cleaning processes concern on the positive effects of the processes only, the stages before and after the cavitation erosion on the metal surface is scarcely researched systematically. In this paper aluminum and steel alloys are impinged by the high pressure cavitation jet with different processing parameters. The surface properties of the alloys, e.g., surface hardness, surface topography and residual stress are tested, and the mechanical characteristics of the alloy surface under different enhancement and destroy stages are analyzed.

1. Experimental Device and Method.

1.1. High-Pressure Cavitation Jet System. A high-pressure water jet experiment system was built, as shown in Fig. 1. The maximum working pressure of the selected plunger pump is 50 MPa, and the flow rate is 15 l/min. Before the fluid medium enters the plunger pump, a Y-type filter is used to remove impurities. The high-pressure hose is connected between the plunger pump and the jet nozzle. In order to control the upstream pressure of the nozzle, the high-pressure pump is powered by an inverter motor.

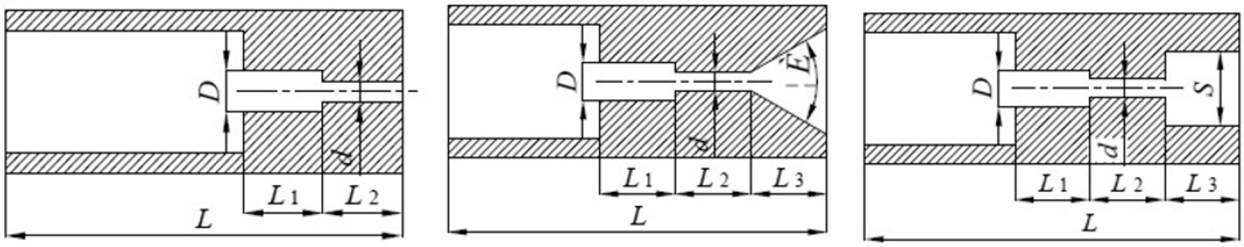

a b c

Fig. 2. Geometry of the nozzles used in the experiment: (a) with no whistle; (b) with a divergent whistle; (c) with a cylindrical whistle.

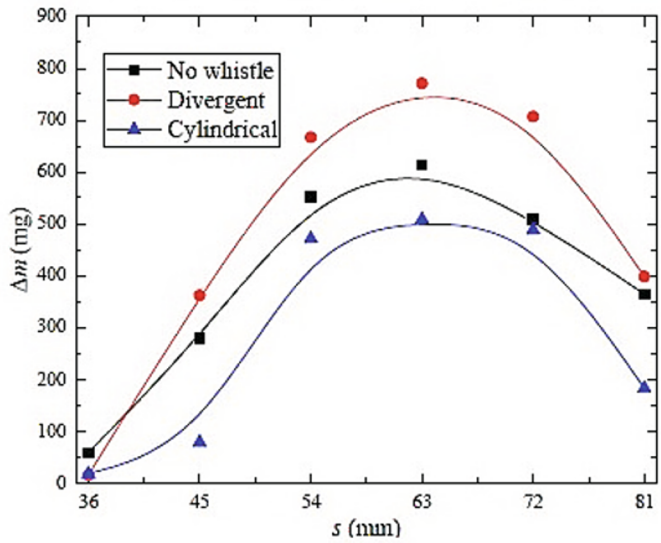

Fig. 3. Mass loss of Al1060 after the jet impingement with different stand-off distances.

The experiments performed in this study mainly involve organ pipe nozzles with different parameters. The main geometric parameters of the organ pipe nozzle include: resonant cavity length L_1, throat length L_2, resonant cavity diameter D and throat diameter d, and outlet shape. The geometry of each nozzle is shown in Fig. 2, where $L_1 = 5$ mm, $L_2 = 44$ mm, $d = 1$ mm, and $\theta = 60°$.

1.2. Experimental Method. The erosion efficiency of the cavitation jet was evaluated by the mass loss of Al1060 before and after the impingement. The metal samples of $100 \times 100 \times 3$ mm dimensions were fixed on a horizontal platform below the nozzle. The target distance between the nozzle and the material is adjusted by controlling the position of the slide above the nozzle. Before the impingement, the samples are polished and ultrasonically cleaned in an ethanol solution, and then fixed on the fixture after drying and weighting. After impingement, clean and dry the samples again and calculate the mass loss finally.

2. Results and Discussion.

2.1. Cavitation Experiment of Pure Aluminum Cavitation Jet.

2.1.1. Influence of Target Distance on Impact Efficiency. The impact performance of different outlet shape organ pipe nozzles is studied at first. In the experiment, the pump pressure is kept as 20 MPa, different stand-off distance is used for the impingement process, and the curve of mass loss versus stand-off distance is obtained, as shown in Fig. 3. It can be seen from the figure that the mass loss increases first and then decreases with the increase of the target distance. For all the three nozzles, the best target distance is $s = 63$ mm.

Comparing the erosion performance of different nozzles, it can be seen that the mass loss of the nozzle without a whistle at a small target distance is slightly larger than that of the other two nozzles. This is because the

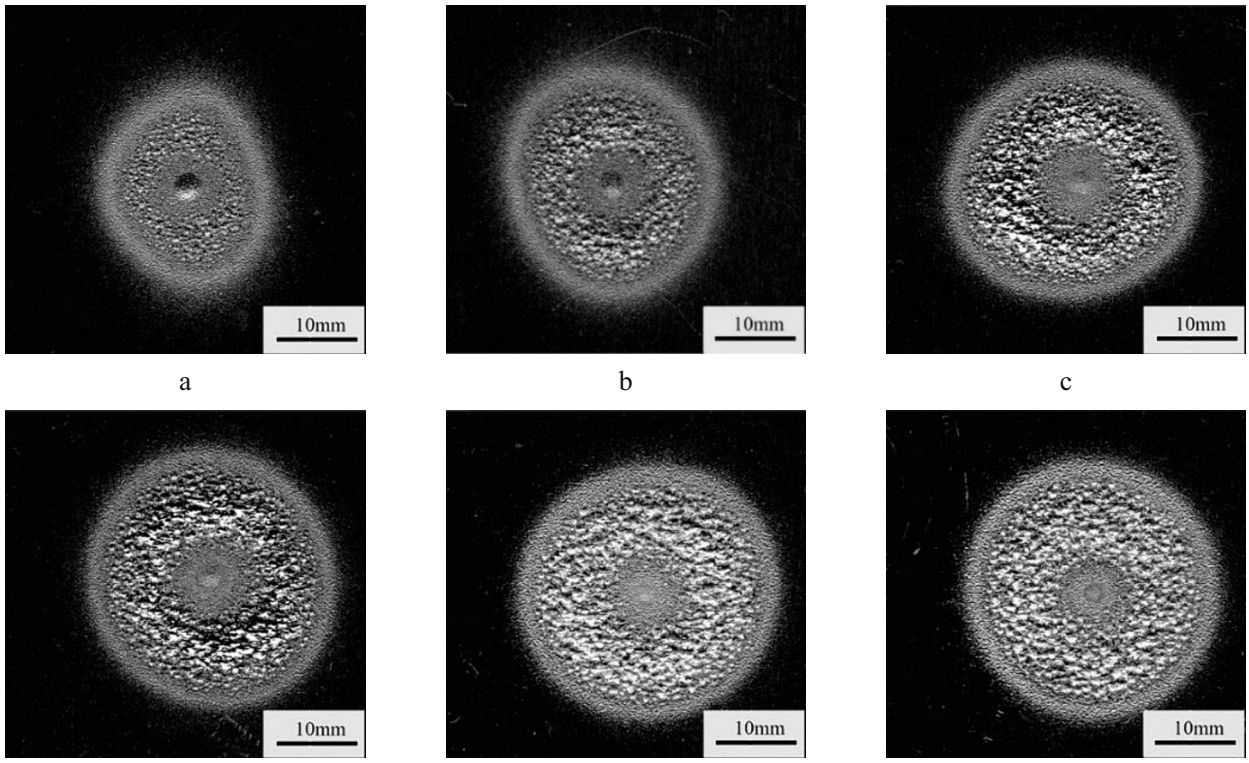

Fig. 4. Surface profile of Al1060 after impingement with different stand-off distance: (a) $s = 36$ mm; (b) $s = 45$ mm; (c) $s = 54$ mm; (d) $s = 63$ mm; (e) $s = 72$ mm; (f) $s = 81$ mm.

cavitation bubbles have not collapsed when they are closed to the wall. With the increase of the target distance, the role of cavitation dominates. Under the optimal distance, the nozzle with a divergent whistle creates a mass loss of 800 mg, the organ pipe nozzle without a whistle creates mass loss of 600 mg and the nozzle with a cylindrical whistle creates a mass loss of 500 mg. Generally, the nozzle outlet shape has a significant impact on the impact performance of the cavitation jet, and the divergent whistle is the optimal outlet form.

Figure 4 shows the surface of Al1060 after impingement by nozzle without whistle at different stand-off distances. The processing parameters are $p = 20$ MPa, $t = 60$ min. As shown in Fig. 4a, at the stand-off distance $s = 36$ mm, the damaged area is small. A pit with a small diameter but a large depth appears in the center, which is created by the high-speed jet. At the outer area is a circular distributed cavitation damage region, which is caused by the shock of the collapsing bubbles. The damaged area increases obviously with the increase of the distance when the stand-off distance is smaller than 63 mm, and the degree of damage increases quickly as well. When the stand-off distance is larger than 63 mm, the damaged area increases slightly and the damaged depth decreases.

The microscopic morphology of Al1060 after 60 min of impact under optimal stand off distance is analyzed. Figure 5 shows the morphology of the sample surface. According to the image after magnification of 500 times, it can be seen that the areas with severe cavitation damage have undulating plastic deformation, which is also covered with circular erosion holes of different shapes and sizes. Each pit represents an effective impact of collapse shock. Due to the long impact time and random distribution of the collapsing position, the cavities overlap and etch pits in the damaged area are connected, causing a large area of material to peel off.

2.1.2. Effect of Processing Time on The Erosion Process. Figure 6 shows the surface morphology of Al1060 after different impact times. The nozzle used for the impact has a divergent outlet. The impact parameters are $p = 20$ MPa, $t = 60$ min, and $s = 63$ mm. It can be seen from Fig. 6a that after 5 min of cavitation jet impingement, a ring-shaped plastic deformation area begins to appear on the surface, and the surface roughness is basically not changed in the circular area with a center diameter of about 100 mm. With a continuous increase in the impact time,

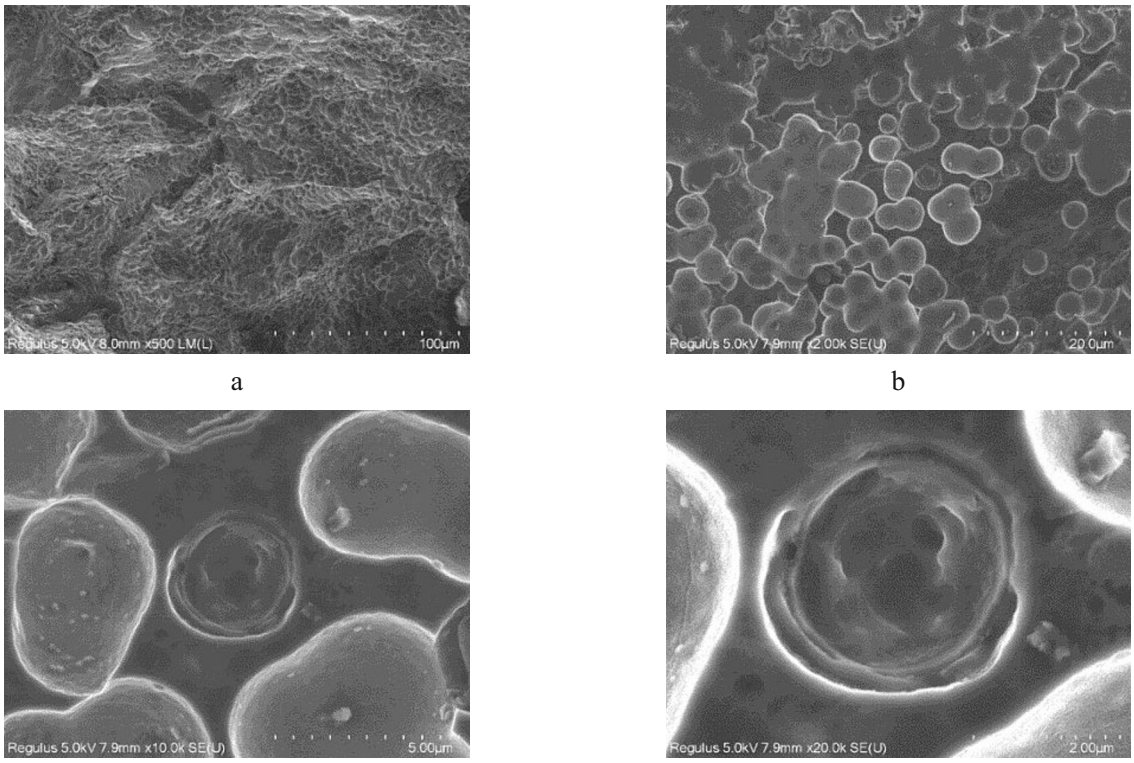

a b c d

Fig. 5. SEM of Al1060 surface after the cavitation jet impingement: (a) ×500; (b) ×5000; (c) ×10000; (d) ×20000.

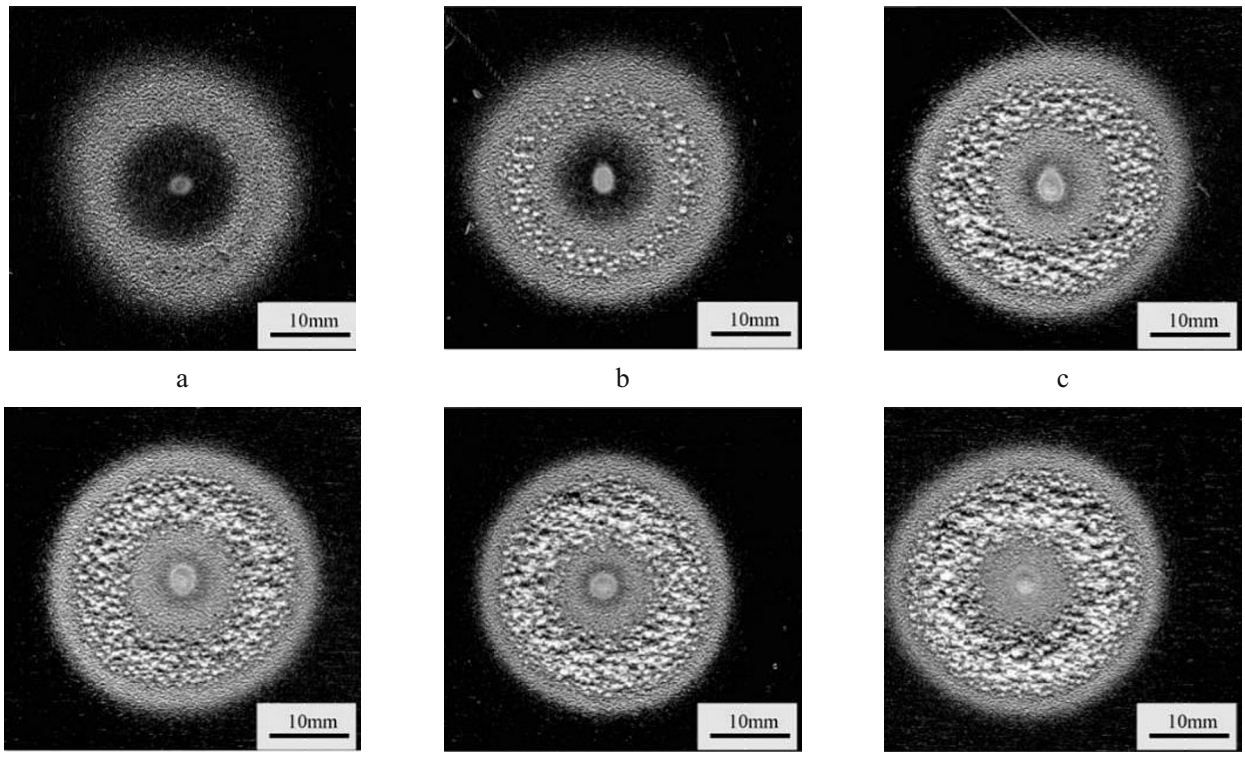

a b c d e f

Fig. 6. Surface morphology of Al1060 after impingement for different times: (a) $t = 5$ min; (b) $t = 10$ min; (c) $t = 20$ min; (d) $t = 30$ min; (e) $t = 40$ min; (f) $t = 50$ min.

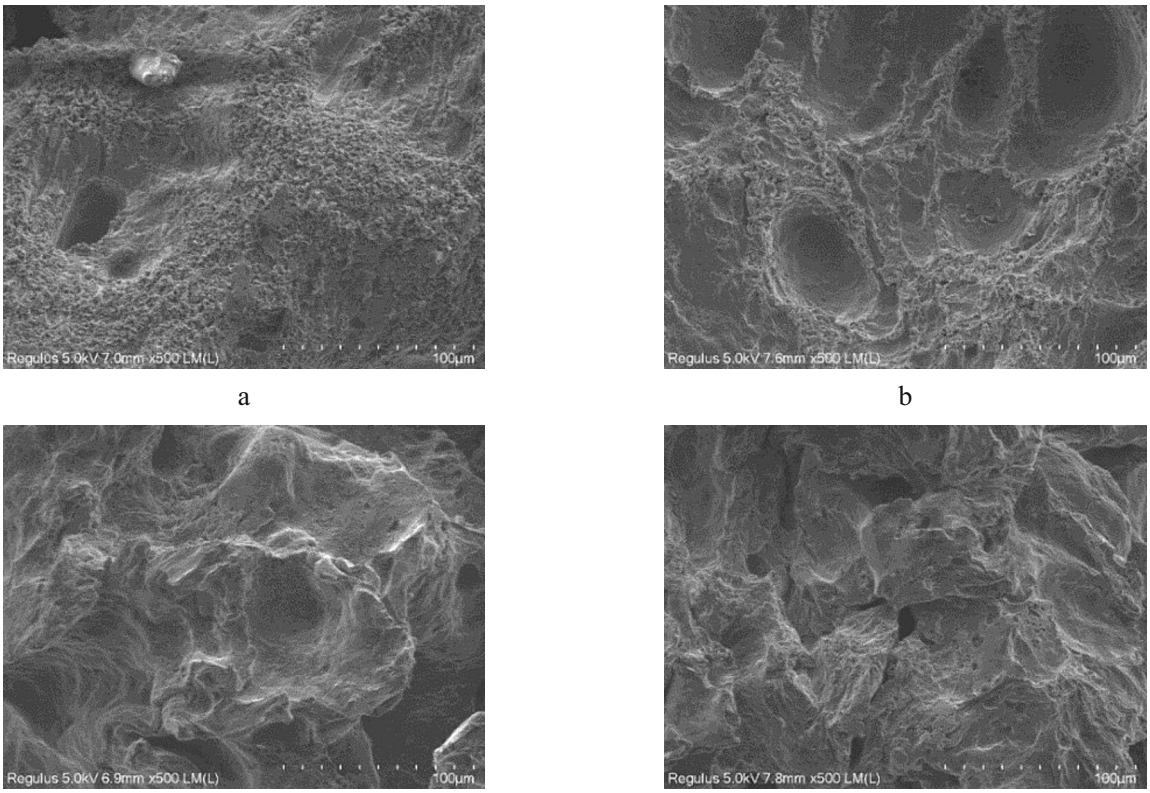

Fig. 7. Surface morphology after cavitating jet impingement with different time: (a) $t = 5$ min; (b) $t = 10$ min; (c) $t = 30$ min; (d) $t = 50$ min.

the central area is also completely deformed, the area of the material surface layer that failed to peel off is gradually increased, and the depth of the pits continues to increase.

In order to show the fracture process of high-pressure water impact jet on the surface of Al1060 material, samples with four different impact times were selected for SEM analysis, and an enlarged image of the surface of the impact destruction area was obtained as shown in Fig. 7. When the cavitation collapses at different positions, impact loads from different directions are generated, further distorting the bulge on the surface of the material. Subsequently, the material enters a stable failure period, when the fatigue failure occurs and the material is continuously peeled off from the surface layer. The material exposed from the cavitation damage pits will continue to undergo fatigue damage under the continuous impact of the cavitation shock. As the impact time increases, the depth of destruction also gradually increased.

2.2. Property Change of Al6061 after Cavitation Jet Impingement. Compared with aluminum alloy Al1060, aluminum alloy Al6061 has an obviously improved hardness and yield strength. In the current research, an Al6061 sample was processed by an organ pipe nozzle with a 60° divergent outlet angle, and the pressure was controlled as 20 MPa. The processing time was 5 and 20 min, respectively.

Figure 8 shows an SEM image of the material after 5 min of cavitation jet processing. As can be seen from Fig. 8a, the surface of the Al6061 material has begun to undergo plastic deformation, resulting in the occurrence of cavitation erosion pits, but the number of pits is small and discretely distributed. Enlarging the image by 2000 times, it can be seen that the edge of the pit is jagged, which is consistent with the hard material's surface peeling characteristics due to fatigue failure. Its inner surface is not a smooth curve, but is covered with irregular polygonal uneven structure. Observing the 10000 times magnified image of the pits, the polygonal concave-convex structure can be observed more clearly. In addition, some granular precipitated phases can be seen in the pits, the color of which is obviously different from that of the main phase of aluminum alloy.

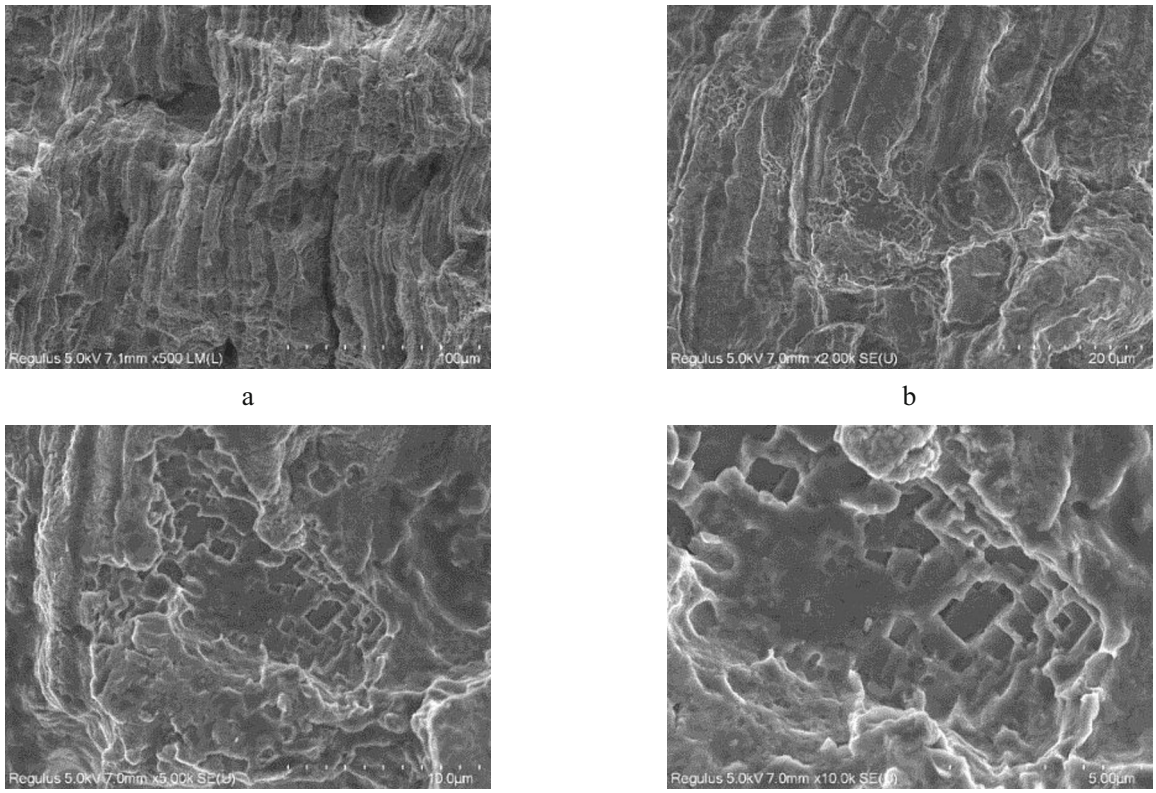

a b c d

Fig. 8. Surface morphology of Al6061 after cavitation jet peening with 5 min: (a) ×500; (b) ×2000; (c) ×5000; (d) ×10000.

Figure 9 shows the SEM image of the Al6061 surface after impact with different target distances. The pressure used for the jet is $p = 20$ MPa, and the processing time is $t = 20$ min. It can be seen that the sample surface corresponding to the 45 mm stand-off distance has undergone significant plastic deformation, and material peeling occurred in some areas. When the stand-off distance is 63 mm, the degree of deformation of the material surface is higher. Observing the sample with an impact target distance of 81 mm, it was found that the surface was relatively smooth, without obvious large fluctuations. At this time, the pits on the surface are relatively dispersed, indicating that the number of cavitation bubbles that reach this location has been reduced, and most cavitation bubbles have collapsed upstream. It can be seen that the maximum impact strength of the nozzle under the above-mentioned processing pressure is 63 mm.

Figure 10 shows the surface hardness of Al6061 after impingement. The stand-off distance is 63 mm, and the processing time is 5 min and 10 min, respectively. The original hardness of the aluminum alloy used is 70 HV. According to the material test results, when the processing time is 5 min, the hardness of the sample gradually decreases in the depth direction. The measured point closest from the surface layer ($s = 0.17$ mm) has a hardness value of 77.42 HV, while at a depth of 2.12 mm, hardness decreases to 71.59 HV. When the processing time is increased to 10 min, the hardness in the section with a depth of less than 0.47 mm has an increasing trend, while the hardness further away from the surface decreases with increasing depth. The hardness value at each position is higher than the case where the processing time is 5 min. The maximum hardness value reaches 82.5 HV. In general, the impact of the cavitation water jet can effectively improve the surface hardness of Al6061, but due to the weak strength of the aluminum alloy material, when the impact time exceeds 10 min, it will start to cause cavitation damage to the surface of the material, and the surface hardness drops again.

The Al6061 samples impinged by the cavitation jet at different target distances were selected for X-ray stress testing. The processing parameters were impact pressure $p = 20$ MPa, impact time $t = 20$ min, the stand-off distances

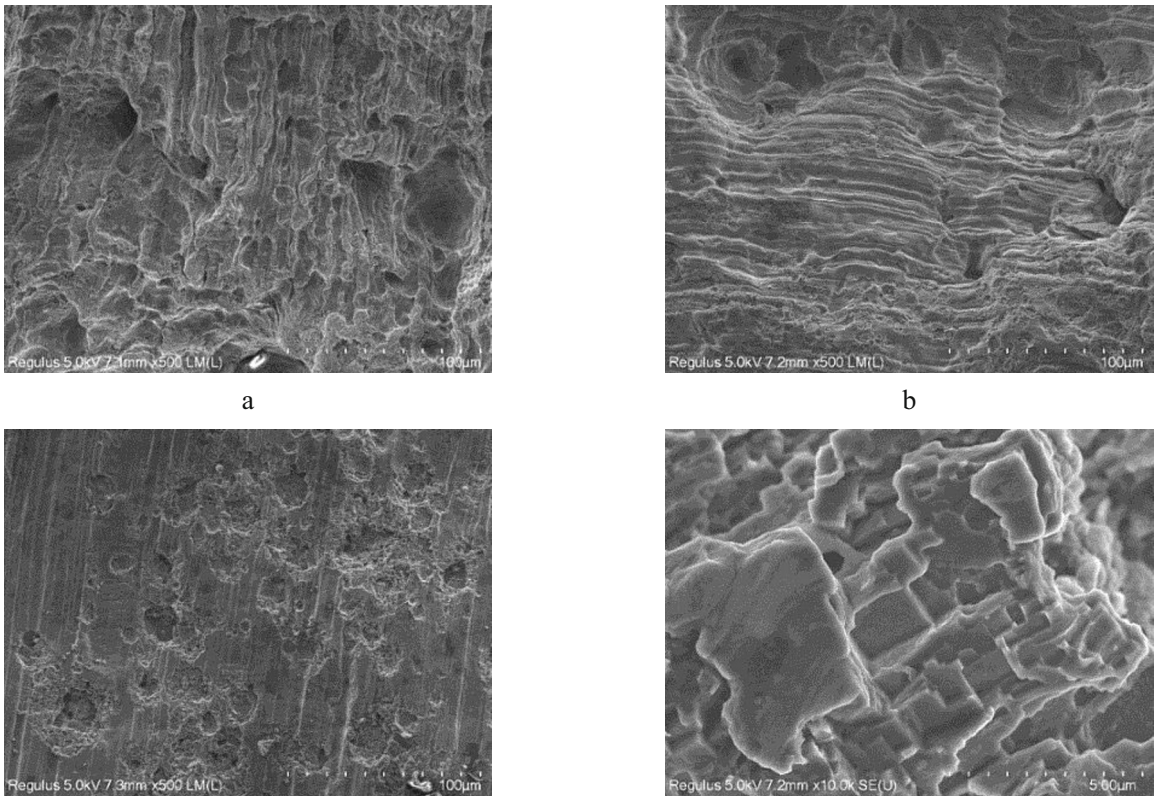

Fig. 9. Surface of Al6061 after cavitation peening with different stand-off distances: (a) 45 mm stand-off distance (×500); (b) 63 mm stand-off distance (×500); (c) 81 mm stand-off distance (×500); (d) 81 mm stand-off distance (×20000).

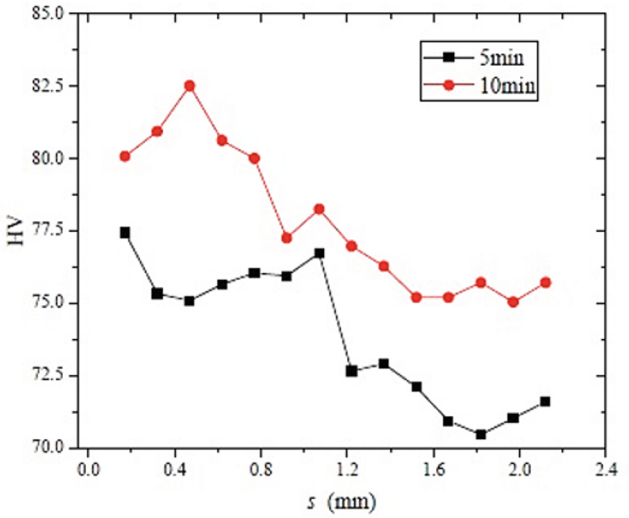

Fig. 10. Hardness of Al6061 after impingement.

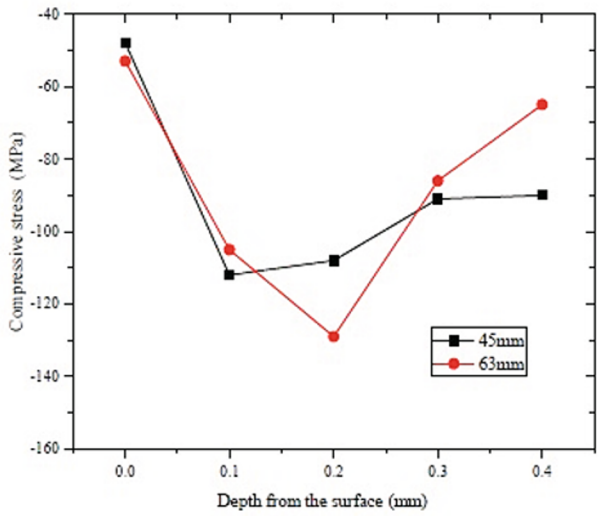

Fig. 11. Residual stress of Al6061 after impingement.

are 36, 63, and 81 mm, respectively. The residual stress distribution obtained from the test is shown in Fig. 11. It can be found that the residual stress of the surface layer of the material has the same trend after impact at the stand-off distance of 45 and 63 mm. The compressive stress is first increased and then decreased, along the direction perpendicular to the surface. From the above research on the influence of target distance on erosion performance, it is

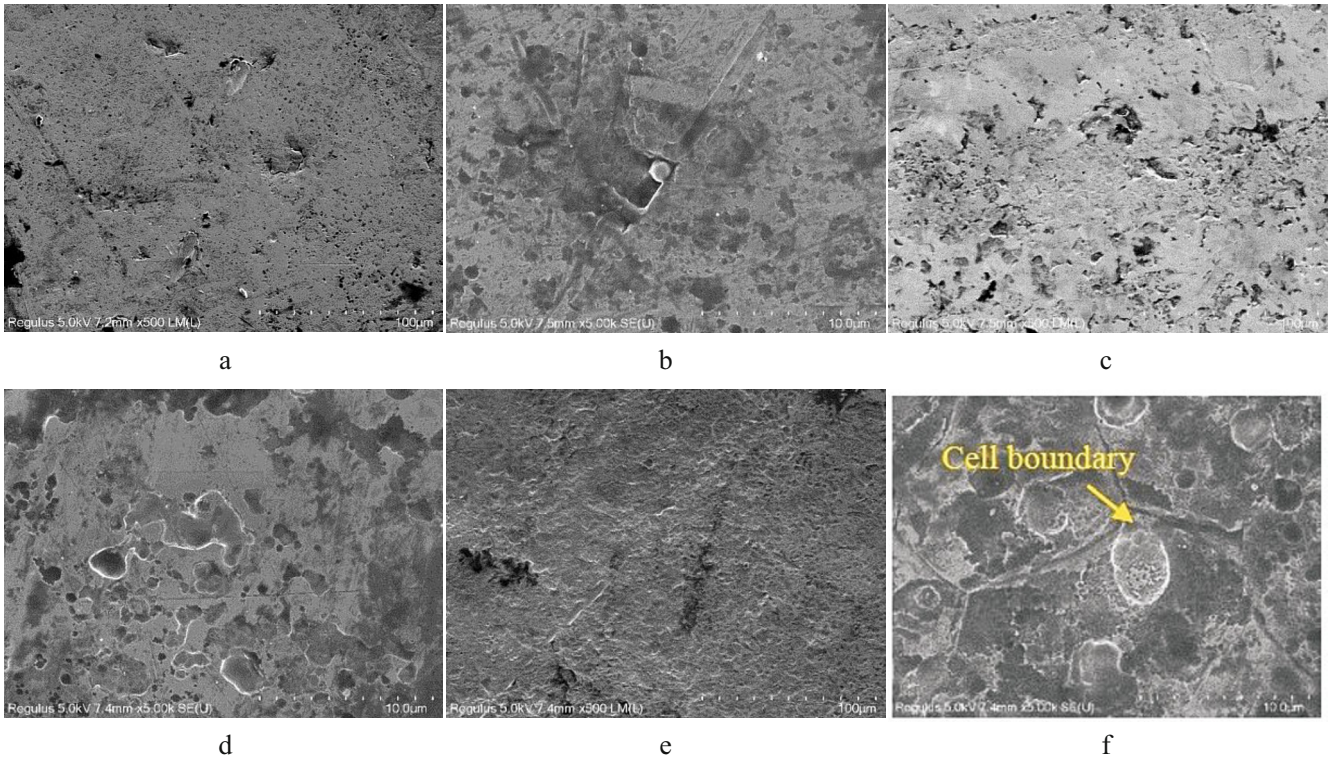

a b c

d e f

Fig. 12. Surface morphology of 304 stainless-steel peened with different times: (a) 5 min (×500); (b) 5 min (×5000); (c) 10 min (×500); (d) 10 min (×5000); (e) 20 min (×500); (f) 20 min (×5000).

known that the nozzle has the stronger impact performance at 63 mm. According to the measurement results of residual stress, it can be found that the residual stress layer has a thickness of 0.2 mm after impact at this target distance, and the maximum value of the compressive stress reaches 129 MPa. When the stand-off distance is 45 mm, the maximum compressive residual stress shows at a depth of 100 μm, and the maximum stress is 112 MPa. It can be seen that the cavitation jet can create obvious residual stress on the surface of the aluminum alloy. Also, the cavitation water jet impact can act to a large depth, and the layer depth of the compressive residual stress can reach more than 400 μm.

2.3. Property Change of 304 Stainless Steel after Cavitation Jet Impingement. 304 stainless steel is widely used in the construction of building materials, chemicals and marine equipment. In this paper, the effect of processing time of cavitation water jet on the properties of 304 stainless steel was investigated experimentally. Firstly, an organ pipe nozzle with an outlet expansion angle of 60° was used to impact stainless steel samples with different processing times of 5, 10, and 20 min, and the target distance was 63 mm.

Figure 12 shows the SEM image of stainless steel after different impact times. It can be found from Fig. 12a that after 5 min of cavitation jet impact, the surface of the stainless steel is basically the same as the original one. Comparing with Fig. 12b, it was found that there were only a few shallow pits on the surface of the material. When the processing time reaches 10 min, the surface roughness of the material increased slightly. According to the SEM image magnified 5000 times, it can be seen that large pits have begun to appear on the surface of the material, but the number of pits is small and still mostly in small size. In addition to the pits, the remaining parts still retain the flatness before impact, indicating that the material has not undergone large-scale plastic deformation at this time. After 20 min of impact, the surface of 304 stainless-steel began to exhibit more obvious plastic deformation, the surface became uneven and the reflectivity became poor. According to the image magnified 5000 times, more pits have appeared on the surface of the stainless steel at this time, and the size of the pits is significantly larger than that when the impact is 10 min. In addition, under the continuous impact, the grain of the stainless-steel surface layer began to deform, and the grain boundaries start to stand out. According to the SEM image, it can be roughly judged that the

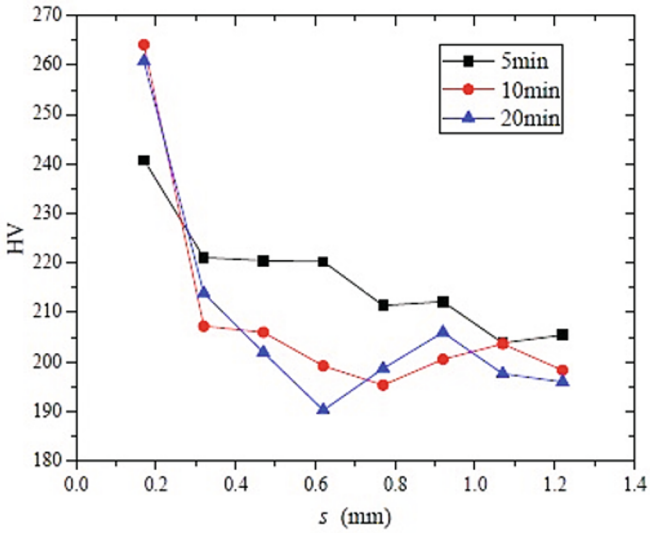

Fig. 13. Hardness distribution of 304 stainless-steel impinged with different time.

impact of the cavitation water jet begins to function after 10 min. When the impact time reaches 20 min, the cavitation load has a greater impact on the grain structure of the surface layer of the stainless-steel material.

The hardness of the stainless-steel samples processed by cavitation jet with different times is experimentally determined, as shown in Fig. 13. The stand-off distance is 63 mm, and the processing pressure is 20 MPa. It can be seen that after impact, 304 stainless steel forms an obvious hard layer from the surface to a depth of 0.3 mm, and as the impact time increases, the surface hardness value continues to increase. After 5 min of cavitation jet impact, the hardness reached 240 HV at 0.2 mm. When the processing time increased to 10 min, the hardness reached 264 HV at 0.2 mm from the surface. When the processing time continued to increase to 20 min, the hardness of the surface layer did not change significantly compared to the situation of 10 min. This is because, during the cavitation impact process, the grains of the 304 stainless steel surface layers are continuously refined, accompanied by slip dislocation between the crystal lattices and the formation of twins. These phenomena have a promoting effect on the increase of the surface hardness of the material. When the grain refinement and dislocation reach a certain level, the impact of the same intensity will no longer have a significant effect on the hardness. At this time, if the continuous cavitation jet impact continues, the surface of the material will begin to undergo plastic deformation and reach the fatigue failure stage. According to the hardness test results, under the above impact parameters, the grain refinement and slip have been fully developed at the impact time of 10 min.

Conclusions. In the current research, high-pressure water jets were used to conduct tests on aluminum alloys Al1060, Al6061, and 304 stainless-steel. The impact performance of cavitation jets was tested by measuring the Al1060 mass loss before and after the impact. The morphology of the materials was observed, and the hardness and residual stress at different depths on the surface of the impacted material were measured. The effect of the cavitation water jet on the material properties was analyzed. The main results from the research are as follows:

1. The outlet shape of the nozzle has a great influence on the impact performance of the cavitation water jet. Among the three outlet shape organ pipe nozzles used in this research, the nozzle with the expanded whistle has the best impact performance, and the optimal stand-off distance of this nozzle is about 63 mm for the jet with a pressure of 20 MPa.

2. Through the impact of the cavitation water jet on Al6061, a hardened layer with a certain thickness is produced on the surface of the aluminum alloy. The hardness of the surface layer gradually decreases from the surface to the depth direction. Through impact, the residual compressive stress of the Al6061 surface layer can reach 129 MPa, and the residual stress depth exceeds 400 μm.

3. After impingement of the cavitation jet, the surface hardness of the 304 stainless-steel increased significantly. When the impact time reached 10 min, the hardness of the surface layer remained nearly unchanged.

When the stainless-steel is processed by the cavitation jet for 20 min, the surface of the material will undergo plastic deformation, indicating that the impact time of 10 min is sufficient for cavitation peening under this processing pressure.

Acknowledgments. This research was funded by the National Natural Science Foundation of China (No. 51979138), Jiangsu Natural Science Research Project (No. 19KJB470029), and Jiangsu Water Conservancy Science and Technology Project (No. 2019038), Nantong Science and Technology Project (No. JC2019155).

REFERENCES

1. M. Hashish, "A modeling study of metal cutting with abrasive waterjets," *J. Eng. Mater. Technol.*, **106**, No. 1, 88–100 (1984).
2. H. Soyama, C. R. Christopher, and M. R. Hill, "Effect of compressive residual stress introduced by cavitation peening and shot peening on the improvement of fatigue strength of stainless steel," *J. Mater. Process. Tech.*, **288**, 116877 (2020), https://doi.org/10.1016/j.jmatprotec.2020.116877.
3. M. Hashish, "A model for abrasive-waterjet (AWJ) machining," *J. Eng. Mater. Technol.*, **111**, No. 2, 154–162 (1989).
4. M. Drzik, L. M. Hlavac, V. Madr, et al., "Relief produced by abrasive water jet and its visualization by contactless optical method," in: Proc. of the SPIE, Vol. 5445, 376–379 (2004), https://doi.org/10.1117/12.560687.
5. M. Hashish, "An investigation of milling with abrasive-waterjets," *J. Eng. Ind.*, **111**, No. 2, 158–166 (1989).
6. M. Hashish, "Characteristics of surfaces machined with abrasive-waterjets," *J. Eng. Mater. Technol.*, **113**, No. 3, 354–362 (1991).
7. S. C. Howard, F. C. Graham, Jr., A. A. Hochrein, et al., *Research and Development of a Cavitating Water Jet Cleaning System for Removing Marine Growth and Fouling from US Navy Ship Hulls*, No. DAI-SCH-7759-001-TR, Daedalean Associates Inc., Woodbine, MD (1978).
8. H. Soyama and M. Mikami, "Improvement of fatigue strength of stainless steel by using a cavitating jet with an associated water jet in water," *Key Eng. Mater.*, **353–358**, 162–165 (2007).
9. H. Soyama, M. Shimizu, Y. Hattori, et al., "Improving the fatigue strength of the elements of a steel belt for CVT by cavitation shotless peening" *J. Mater. Sci.*, **43**, No. 14, 5028–5030 (2008).
10. H. Soyama and F. Takeo, "Comparison between cavitation peening and shot peening for extending the fatigue life of a duralumin plate with a hole," *J. Mater. Process. Tech*., **227**, 80–87 (2016).
11. H. Soyama, T. Kusaka, and M. Saka, "Peening by the use of cavitation impacts for the improvement of fatigue strength," *J. Mater. Sci. Lett.*, **20**, No. 13, 1263–1265 (2001).
12. H. Soyama and D. O. Macodiyo, "Fatigue strength improvement of gears using cavitation shotless peening," *Tribol. Lett.*, **18**, No. 2, 181–184 (2005).
13. H. Soyama and Y. Sekine, "Sustainable surface modification using cavitation impact for enhancing fatigue strength demonstrated by a power circulating-type gear tester," *Int. J. Sustain. Eng.*, **3**, No. 1, 25–32 (2010).
14. D. O. Macodiyo and H. Soyama, "Optimization of cavitation peening parameters for fatigue performance of carburized steel using Taguchi methods," *J. Mater. Process. Tech.*, **178**, 234–240 (2006).
15. Y. Sekine and H. Soyama, "Evaluation of the surface of alloy tool steel treated by cavitation shotless peening using an eddy current method," *Surf. Coat. Technol.*, **203**, No. 16, 2254–2259 (2009).
16. A. Marcon, S. N. Melkote, and M. Yoda, "Effect of nozzle size scaling in co-flow water cavitation jet peening," *J. Manuf. Process*., **31**, 372–381 (2018).
17. M. Ijiri, D. Shimonishi, D. Nakagawa, et al., "New water jet cavitation technology to increase number and size of cavitation bubbles and its effect on pure Al surface," *Int. J. Lightweight Mater. Manuf.*, **1**, No. 1, 12–20 (2018).